Thermodynamic characterization of a tetrahaem cytochrome isolated from a facultative aerobic bacterium, *Shewanella frigidimarina*: a putative redox model for flavocytochrome c_3

Miguel PESSANHA*, Ricardo O. LOURO*, Ilídio J. CORREIA*, Emma L. ROTHERY†, Kate L. PANKHURST†, Graeme A. REID‡, Stephen K. CHAPMAN†, David L. TURNER§ and Carlos A. SALGUEIRO*¶[1]

*Instituto de Tecnologia Química e Biológica, Universidade Nova de Lisboa, Rua da Quinta Grande 6, 2780-156 Oeiras, Portugal, †Department of Chemistry, University of Edinburgh, West Mains Road, Edinburgh EH9 3JJ, Scotland, U.K., ‡Institute of Cell and Molecular Biology, University of Edinburgh, Mayfield Road, Edinburgh EH9 3JR, Scotland, U.K., §Department of Chemistry, University of Southampton, Southampton SO17 1BJ, U.K., and ¶Departamento de Química da Faculdade de Ciências e Tecnologia da Universidade Nova de Lisboa, Quinta da Torre, 2829-516 Caparica, Portugal

The facultative aerobic bacterium *Shewanella frigidimarina* produces a small *c*-type tetrahaem cytochrome (86 residues) under anaerobic growth conditions. This protein is involved in the respiration of iron and shares 42 % sequence identity with the N-terminal domain of a soluble flavocytochrome, isolated from the periplasm of the same bacterium, which also contains four *c*-type haem groups. The thermodynamic properties of the redox centres and of an ionizable centre in the tetrahaem cytochrome were determined using NMR and visible spectroscopy techniques. This is the first detailed thermodynamic study performed on a tetrahaem cytochrome isolated from a facultative aerobic bacterium and reveals that this protein presents unique features. The redox centres have negative and different redox potentials, which are modulated by redox interactions between the four haems (covering a range of 8–56 mV) and by redox–Bohr interactions between the haems and an ionizable centre (-4 to -36 mV) located in close proximity to haem III. All of the interactions between the five centres are clearly dominated by electrostatic effects and the microscopic reduction potential of haem III is the one most affected by the oxidation of the other haems and by the protonation state of the molecule. Altogether, this study indicates that the tetrahaem cytochrome isolated from *S. frigidimarina* (*Sfc*) has the thermodynamic properties to work as an electron wire between its redox partners. Considering the high degree of sequence identity between *Sfc* and the cytochrome domain of flavocytochrome c_3, the structural similarities of the haem core, and that the macroscopic potentials are also identical, the results obtained in this work are rationalized in order to put forward a putative redox model for flavocytochrome c_3.

Key words: electron transfer protein, multihaem, NMR, paramagnetic shift.

INTRODUCTION

The respiratory processes in bacteria are extremely flexible and diverse, reflecting the ability of these micro-organisms to adapt to a variety of environments, with a major impact in the global environment including central roles in several biogeochemical cycles [1–3]. Intimately correlated with the bacterial respiratory flexibility, Nature has selected different electron transfer proteins that modulate the spatial disposition of the cofactors and their affinity for electrons [4]. Multihaem proteins in general, and small tetrahaem cytochromes in particular, are good examples of such selectivity and modulation of the properties of redox centres by protein polypeptide chains and have been studied extensively as model proteins [5–7].

All small monomeric tetrahaem cytochromes described in the literature during the last decades were isolated from anaerobic bacteria belonging to the Desulfovibrionacea family and contain approx. 30 residues per haem group [6,8–11]. Ensembles of only four haem groups are also found in much larger and complex proteins such as in the N-terminal domain of flavocytochromes c_3 [12,13], in the tetrahaem cytochrome subunit of the *Rhodopseudomonas viridis* photosynthetic reaction centre [14] and also in cytochrome c_{554}, isolated from *Nitrosomonas europaea* ([15,16] and references therein).

The finding of a small tetrahaem cytochrome in a facultative aerobic bacterium belonging to the *Shewanella* genus revealed that this type of electron transfer protein is more widespread in Nature than previously thought and that these proteins may play a fundamental and ubiquitous role in the bacterial bioenergetic processes [17–19].

Shewanella spp. constitutes a remarkable example of respiratory flexibility, with the capacity to use a variety of compounds, including insoluble minerals, as terminal electron acceptors [20,21]. *Shewanella* bacteria respiring on Fe(III) must surpass the difficulty inherent in the use of a respiratory compound with a low solubility in aqueous solutions [e.g. Fe (hydr)oxides] at physiological pH values. Apparently, these bacteria overcome this problem by releasing soluble quinones that can carry electrons from the cell surface to Fe(III) oxide [22,23] and by producing a variety of multihaem *c*-type cytochromes, located in the periplasmic space and outer membrane [24–29]. The precise mechanism of Fe(III) reduction and its

Abbreviations used: NOESY, nuclear Overhauser enhancement spectroscopy; *Sfc*, *Shewanella frigidimarina* NCIMB400 tetrahaem cytochrome; *Sffcc*$_3$, *Shewanella frigidimarina* NCIMB400 flavocytochrome c$_3$; *Soc*, *Shewanella oneidensis* MR-1 tetrahaem cytochrome.

[1] To whom correspondence should be addressed, at the Instituto de Tecnologia Química e Biológica, Universidade Nova de Lisboa (e-mail cas@itqb.unl.pt).

connection with such multihaem cytochromes are not yet elucidated. However, it was shown by gene disruption that a small tetrahaem cytochrome isolated from *Shewanella frigidimarina* NCIMB400 (*Sfc*) containing only 86 residues is indeed involved in iron respiration [18].

The solution structure of the haem core, the specific axial ligands and the haem order of oxidation of the haems in *Sfc* were determined by NMR spectroscopy [30]. The linear architecture and topology of the *Sfc* haem groups are similar to that found in the flavocytochrome c_3 N-terminal cytochrome domain of *S. frigidimarina* NCIMB400 flavocytochrome c_3 (*Sffcc*$_3$) [13], a 63.8 kDa periplasmic enzyme with unidirectional fumarate reductase activity [31], isolated from *S. frigidimarina*. It is also displayed in four of the five haem groups of the NrfA-type nitrite reductase isolated from *Sulfurospirillum deleyianum* [32] and hydroxylamine oxidoreductase [33].

The occurrence of interactions between the closely arranged redox centres (homotropic co-operativity) in the multihaem cytochromes c_3 from sulphate-reducing bacteria has been described [34–42]. Heterotropic co-operativity, involving modulation of the haem microscopic reduction potentials by pH changes (redox–Bohr effect), has also been reported for these proteins [34–42]. This network of redox and redox–Bohr co-operativities allows type I tetrahaem cytochromes c_3 from sulphate-reducing bacteria to couple the transfer of electrons and protons, performing energy transduction [39,43]. To study such co-operative mechanisms in multicentre electron transfer proteins, it is necessary to obtain thermodynamic information for each redox centre. Our current ability to conduct a detailed analysis of the microscopic redox properties of multihaem proteins relies on NMR data and is limited to the analysis of small proteins [36,39,40,42,44]. This is a consequence of the degradation of spectral quality as the molecular mass increases and/or of the dramatic increase in the number of experimental parameters to be determined as the complexity of the system increases.

This study presents the first detailed thermodynamic characterization of a tetrahaem cytochrome isolated from facultative aerobic bacteria. The thermodynamic properties observed for *Sfc* are rationalized in terms of a putative redox functional model for flavocytochrome c_3 isolated from the same micro-organism.

MATERIALS AND METHODS

Bacterial growth and protein purification

S. frigidimarina NCIMB400 cells were grown and tetrahaem cytochrome was purified as described previously [18].

NMR sample preparation

For NMR experiments the protein was lyophilized twice with ^2H_2O (99.9% atom) and then dissolved in approx. 500 μl of ^2H_2O (99.96% atom) to a final concentration of 1 mM. Identical NMR spectra (results not shown) were obtained before and after the lyophilization, showing that the protein structure was not affected.

The ionic strength was adjusted to approx. 100 mM by addition of NaCl in ^2H_2O. The pH was adjusted by addition of small amounts of NaO^2H or ^2HCl. In the reduced and intermediate stages of oxidation the pH was adjusted inside an anaerobic glove box (Mbraun MB 150 I) with argon circulation to avoid reoxidation of the sample. The pH values reported are direct meter readings without correction for the isotope effect [45]. Complete reduction of the sample was achieved by the reaction with gaseous hydrogen in the presence of catalytic amounts of the enzyme hydrogenase (isolated from *Desulfovibrio gigas* and *Desulfovibrio vulgaris*). Partially oxidized samples were obtained by first flushing out the hydrogen from the reduced sample with argon and then adding controlled amounts of air into the NMR tube with a syringe through the serum caps.

NMR spectroscopy of partially oxidized samples

All ^{1}H-NMR spectra were obtained in a 500 MHz Bruker DRX500 spectrometer equipped with a 5 mm inverse detection probe head with internal B_0 gradient coils and a Eurotherm 818 temperature-control unit.

To establish the complete pattern of oxidation for each haem methyl group at each pH, several nuclear Overhauser enhancement spectroscopy (NOESY) experiments with 25 ms mixing time and rotating-frame Overhauser enhancement spectroscopy ('ROESY') experiments with 10 ms spin-lock pulse were collected. In each type of spectrum, 4096 (t_2) × 1024 (t_1) data points were recorded, spanning a sweep width of 38 kHz, with 128 scans/increment.

Due to the difficulty in distinguishing some of the haem methyl groups unequivocally at earlier stages of oxidation, NOESY spectra were also acquired with a sweep width of 9 kHz. In these experiments equilibrium was established between molecules completely reduced and molecules with only one haem reduced. Using a smaller sweep width, the spectra digital resolution increases and the signals of the haem methyl groups in earlier stages of oxidation were easier to identify. The NOESY experiments in the intermediate states of oxidation were performed at 298 K in the pH range 5.5–8.5. In all experiments a selective pulse of 800 ms was used for water pre-saturation.

Chemical shifts are reported in parts per million (p.p.m.), and the proton spectra were calibrated using the water signal as an internal reference. All values are reported relative to tetramethylsilane.

The XEASY program [46] was used to visualize the two-dimensional NMR spectra obtained.

Redox titrations followed by visible spectroscopy

Anaerobic redox titrations followed by visible spectroscopy were performed as described previously [40] with approx. 8 μM protein solutions in 100 mM Tris/maleate buffer at pH 6.9 and 7.9. For each pH value the redox titrations were repeated three times to ensure reproducibility, in both oxidative and reductive directions to check for hysteresis. To ensure a good equilibrium between the redox centres and the working electrode [47], a mixture of the following redox mediators was added to the protein solution, all at approx. 2 μM final concentration: Methylene Blue, gallocyanine, Indigo Tetrasulphonate, Indigo Trisulphonate, Indigo Disulphonate, anthraquinone-2,7-disulphonate, 2-hydroxy-1,4-naphthoquinone, anthraquinone-2-sulphonate, safranine O, diquat, benzylviologen, Neutral Red and methylviologen.

The solution potentials were measured using a combined Pt/Ag/AgCl electrode, and the visible spectra were recorded at 298 ± 1 K in a Shimadzu UV-1203 spectrophotometer, placed inside an anaerobic glove box.

The reduced fraction of the *Sfc* was determined using the α band peak at 552 nm. The optical contribution of the mediators was subtracted by measuring the height of the peak at 552 nm relative to the straight line connecting the two isosbestic points (542 and 560 nm) flanking the α band according to the method of Catarino [48].

Thermodynamic modelling

The thermodynamic model developed by Turner et al. [36], which considers five interacting charged centres, four haem groups and one ionizable centre, was used to fit simultaneously the NMR and visible data set. This thermodynamic model defines the energies of oxidation of the four haems and the energy of deprotonation of one acid–base centre. These are further modulated by pairwise interaction energies among the various charged ligands of the macromolecule. Thus such a model is independent of the structure of the macromolecule and of the chemical nature of the ligands, which makes it generally applicable. The model was successfully applied to the study of proteins of various degrees of complexity: four haems and one ionizable centre [36,37,39,42], four haems and two ionizable centres [40] and three haems and one ionizable centre [49], showing the broad applicability of the model.

RESULTS

NMR spectra of partially oxidized samples of *Sfc* show that this protein exhibits fast intramolecular and slow intermolecular electron-exchange rates on the NMR time scale under the experimental conditions used. In fact, any haem substituent displays five discrete NMR signals, which correspond to each of the five possible macroscopic oxidation stages that comprise microstates with the same number (0–4) of oxidized haems [34,36,50]. Under these experimental conditions, the paramagnetic chemical shift of each haem substituent in each oxidation stage is directly proportional to the degree of oxidation of that particular haem [34] and can be used to monitor the oxidation of the haem throughout the redox titration. However, haem substituents that are close to neighbouring haem groups have an additional contribution to their observed chemical shifts due to the oxidation of the neighbouring haems (the extrinsic paramagnetic shifts) and consequently are not suitable to follow haem oxidation. In the present study, the haem methyl groups $18^1CH_3^{I}$, $12^1CH_3^{II}$, $2^1CH_3^{III}$ and $18^1CH_3^{IV}$ (Roman numerals indicating the haem by the order of attachment to the polypeptide chain) were chosen to follow the individual haem oxidation since these substituents were shown to have negligible extrinsic con-

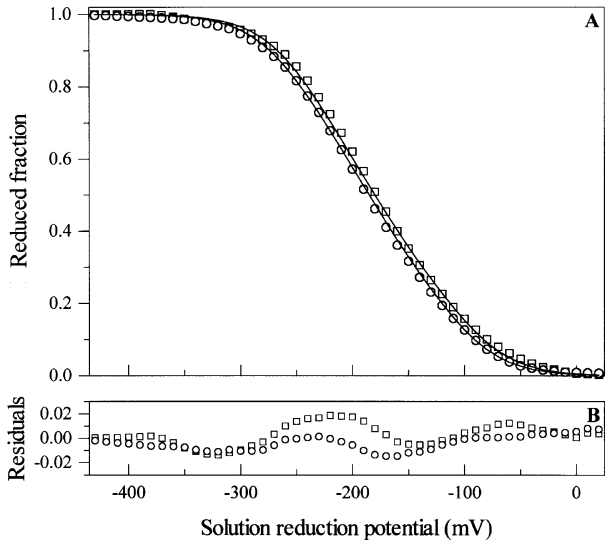

Figure 2 Reduced fraction of *Sfc* determined by visible spectroscopy at pH 6.9 (□) and 7.9 (○)

(**A**) Solid lines are the result of the simultaneous fitting of the NMR (see Figure 1) and visible data. (**B**) Reduced fraction residuals for each curve represented in (**A**).

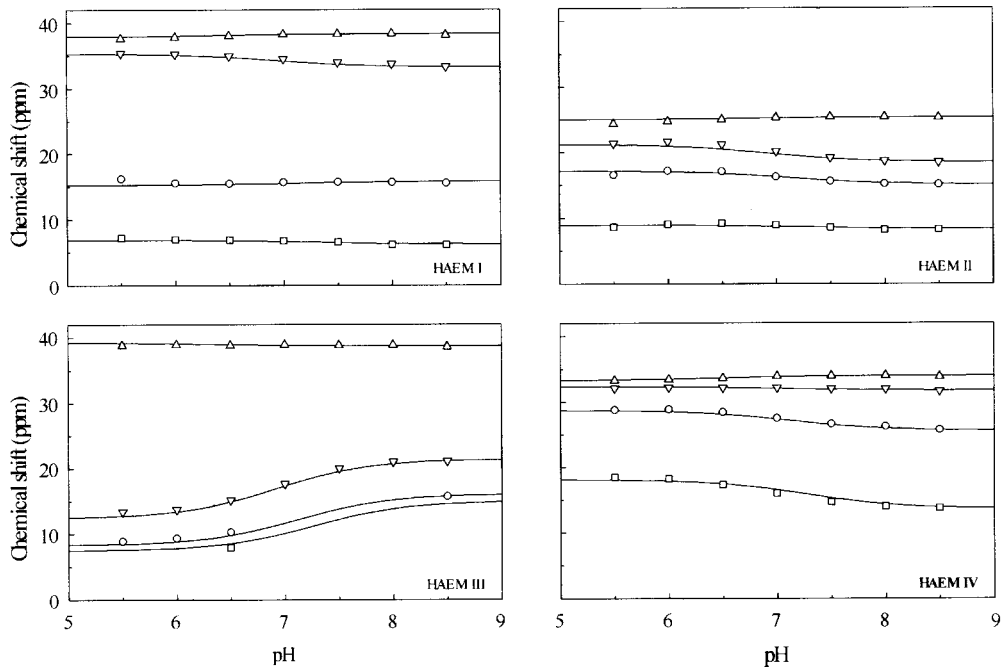

Figure 1 The pH dependence of the chemical shift of haem methyl group resonances $18^1CH_3^{I}$, $12^1CH_3^{II}$, $2^1CH_3^{III}$ and $18^1CH_3^{IV}$ of *Sfc*

□, Stage 1 of oxidation; ○, stage 2; ▽, stage 3; △, stage 4. The chemical shift of the haem methyl groups in the fully reduced stage are not plotted since they are unaffected by pH. Chemical shifts are 3.24 ($18^1CH_3^{I}$), 3.52 ($12^1CH_3^{II}$), 1.89 ($2^1CH_3^{III}$) and 3.32 ($18^1CH_3^{IV}$) p.p.m.

Table 1 Thermodynamic parameters determined for *Sfc* by fitting the NMR and visible data to the model of charged interacting centres

(**A**) Diagonal terms (in bold) represent the oxidation energies of the four haems and the deprotonating energies for the ionizable centre in the fully reduced and protonated protein. The off-diagonal elements represent the redox and redox–Bohr interaction energies between the five centres. Standard errors are given in parentheses. (**B**) *Sfc* macroscopic pK_a values for the five stages of oxidation, from the fully reduced protein (stage 0) to the fully oxidized (stage 4).

(**A**)

	Energy (meV)				
	Haem I	Haem II	Haem III	Haem IV	Ionizable centre
Haem I	**−190(3)**	22(1)	11(1)	9(1)	−9(2)
Haem II		**−212(3)**	56(2)	8(1)	−11(2)
Haem III			**−199(3)**	42(2)	−36(2)
Haem IV				**−229(2)**	−4(2)
Ionizable centre					**443(5)**

(**B**)

pK_a				
Stage 0	Stage 1	Stage 2	Stage 3	Stage 4
7.5	7.3	7.1	6.9	6.5

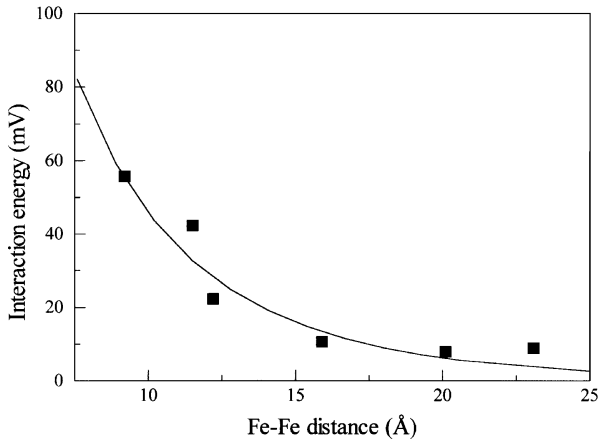

Figure 3 Distance dependence of the pairwise interaction energies between the iron centres

The line was calculated for an exponentially decaying Coulomb interaction considering an effective dielectric constant of 8.6 (0.6; S.E.) and Debye length of 7.7 (0.3) Å.

tributions to their chemical shifts [30]. Thus the percentages of oxidation at pH 6.5 and 298 K [30] in each stage of oxidation were 10.5 % (stage 1), 35.3 % (stage 2) and 91.2 % (stage 3) for haem I; 26.4 %, 63.1 % and 82.2 % for haem II; 16.4 %, 22.7 % and 36.0 % for haem III; and 46.2 %, 83.0 % and 95.2 % for haem IV.

The pH dependence of the paramagnetic chemical shifts of each haem methyl group in the pH range 5.5–8.5, and the data obtained for redox titrations followed by visible spectroscopy at pH 6.9 and 7.9, were used to monitor the thermodynamic properties of *Sfc*.

The fittings of both NMR and visible data are reported in Figures 1 and 2, respectively. The experimental uncertainty of the NMR data was estimated from the line width of each NMR signal, and the visible data points were given an uncertainty of 3 % of the total optical signal. The thermodynamic parameters obtained for *Sfc* are listed in Table 1, together with the macroscopic pK_a values for the five stages of oxidation.

DISCUSSION

The quality of the fittings obtained for the pH dependence of the paramagnetic chemical shifts of the methyl groups (Figure 1), and the redox titrations followed by visible spectroscopy (Figure 2), clearly shows that the thermodynamic model used is appropriate to describe the properties of *Sfc*. The thermodynamic parameters obtained show that the microscopic reduction potentials of each haem are negative, as expected for bis-histidinyl-ligated haem groups exposed to the solvent ([51] and references therein). The interaction energy for each pair of haems is positive, indicating that the oxidation of a particular haem renders the oxidation of its neighbours more difficult (negative homo-cooperativity). On the other hand, the interaction energies between the haems and the acid–base centre are negative (positive hetero-cooperativity), i.e. the oxidation of the haems facilitates the deprotonation of the acid–base centre, and vice versa.

Since the spatial arrangement of the four haems in the structure is known [30], the magnitude of the interaction energy between each pair of haems can be correlated with the respective distance (Figure 3). Considering the interactions as shielded electrostatic effects [52], experimental data were fitted with an effective dielectric constant of 8.6 (0.6; S.E.) and Debye length of 7.7 (0.3) Å. Although empirical, both these values are within a reasonable range for the experimental conditions used [53]. The quality of the fit obtained clearly indicates that electrostatic effects rather than conformational changes between redox stages dominate all pairwise interaction energies between the haems.

The analysis of the relative microscopic reduction potentials of each haem group (Table 1A) shows that haem IV has the lowest redox potential in the reduced and protonated protein, followed by haems II, III and I. However, the negative homo-cooperativities between the haem groups alter the affinity of each redox centre along the oxidation steps of the cytochrome such that their apparent midpoint reduction potentials (i.e. the point at which the oxidized and reduced fractions of each haem group are equally populated), E_m^{app}, vary. In fact, the order of the apparent midpoint reduction potentials is IV, II, I, III (Figure 4A). The profile of oxidation of the haem groups is shown in Figure 4, where several crossovers between the individual curves occur, clearly indicating that the affinity of each redox centre is tuned by neighbouring haem groups. The effect of the negative homo-cooperativities between haem groups is particularly marked for haem III. Indeed, it has redox interactions of 11, 56 and 42 mV with haems I, II and IV, respectively, which lead to an increase in the reduction potential of 109 mV as oxidation of the other haems progresses. Thus the oxidation profile of this haem is affected extensively by the oxidation of neighbouring haems so that it becomes the haem with highest E_m^{app} (Figure 4).

The comparison of individual haem oxidation profiles calculated for different pH values show that the relative order for E_m^{app} remains unaltered in the pH range 5.5–8.5 (Figure 4). Nonetheless, the oxidation profile of each haem group in the early stages of oxidation is clearly affected by pH, reflecting mainly the modulation of the microscopic reduction potential of haem III. In fact, the oxidation curve of haem III is most affected by pH due to it having the highest heterotropic co-operativity, which also suggests that the ionizable centre is located close to this haem group (Table 1A). Consequently, the E_m^{app} of haem III

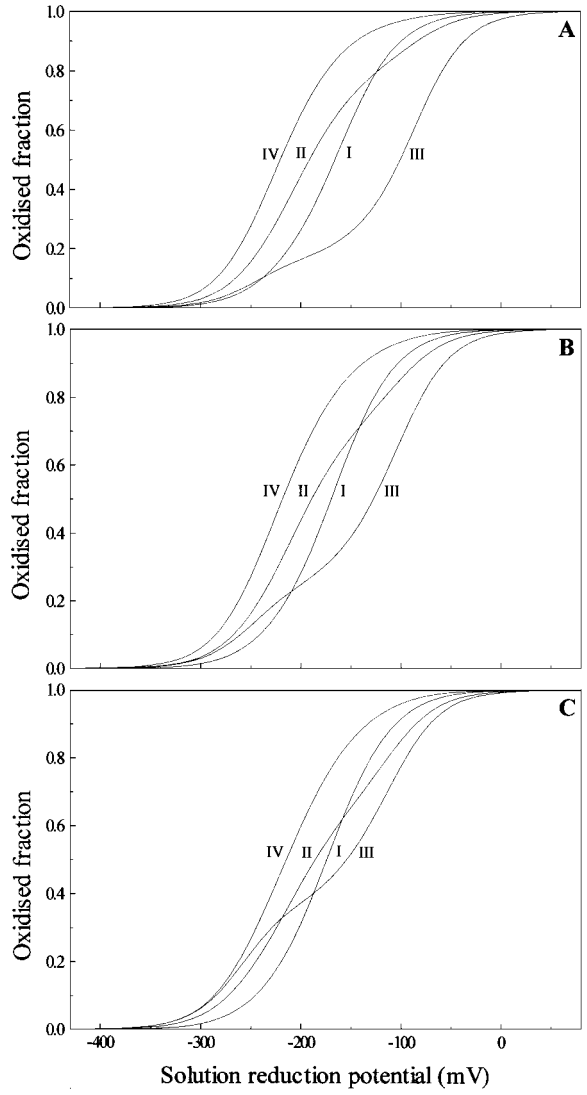

Figure 4 Oxidized fractions of the individual haems of *Sfc* at pH 5.5 (A), 7.0 (B) and 8.5 (C)

The curves were calculated as a function of the solution reduction potential using the parameters listed in Table 1.

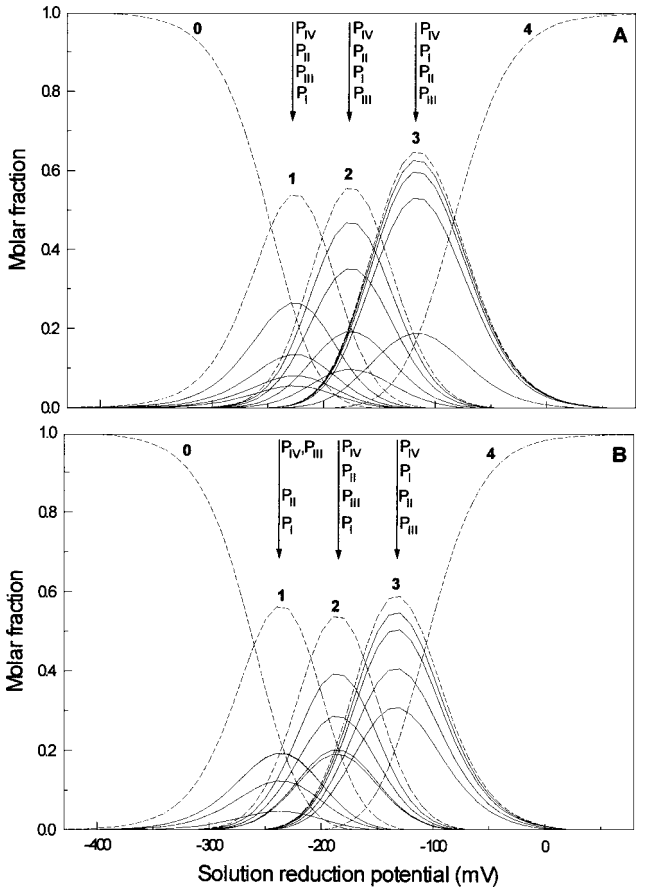

Figure 5 Total and individual haem populations of the five redox oxidation states (0–4) for *Sfc* at pH 5.5 (A) and 8.5 (B)

The curves were calculated as a function of the solution reduction potential using the parameters listed in Table 1. Dashed lines indicate the sum of the populations of each microstate in each oxidation stage. Solid lines indicate the total population, P_i, of the microstates in which haem I, II, III or IV is oxidized (i = I–IV) in the intermediate oxidation stages (1–3). Arrows are labelled from top to bottom according to the magnitude of the different P_i values.

approaches that of the other haem groups as the solution pH increases (Figure 4). The pH control of the electron affinity of haem III also has a dramatic effect on the overall population of each intermediate oxidation stage (Figure 5). Indeed, the relative populations with haem III oxidized in the fully protonated protein (Figure 5A) are much smaller than those in the fully deprotonated protein (Figure 5B). Altogether, the thermodynamic results obtained for *Sfc* and the important homo- and hetero-cooperativities displayed by haem III indicate that this haem plays an important role in the redox cycle of this electron transfer protein.

The analysis of the redox titrations, followed by visible spectroscopy at pH 6.9 and 7.9, shows a small separation between the two curves (approx. 5 mV; Figure 2). Thus the global redox–Bohr effect is small, with only 1 pH unit between the fully reduced and fully oxidized protein pK_a values (Table 1B), and the macroscopic reduction potentials of the cytochrome are essentially unaffected by the pH (Figure 6).

Recently, the crystal structure for both oxidized and reduced forms of a homologous small *c*-type cytochrome, isolated from *Shewanella oneidensis* MR-1 (*Soc*) [54], was reported. This cytochrome shares 69% sequence identity with *Sfc* and the structure showed that the haem core architecture of the tetrahaem cytochrome isolated from *Soc* is very similar to that previously reported for *Sfc* [30]. Due to the high solvent accessibility and the close interaction with the negatively charged Glu-31, it was proposed that haem I in *Soc* is most likely to have one of the lowest redox potentials of the four haem groups [54]. However, as pointed out by the authors, other effects may counteract the influence of the high solvent accessibility [54]. From our results on *Sfc*, the order of oxidation measured experimentally is IV, II, I and III, which is different from that proposed for *Soc*. Thus a definitive comparison between the haem microscopic reduction potential of *Soc* and *Sfc* will require a complete thermodynamic characterization of *Soc* with structural assignment of the NMR signals of the individual haems.

As noted above, the *Sfc* haem core architecture has similarities with the N-terminal cytochrome domain of flavocytochrome c_3 isolated from the same bacterium, except in the position of haem IV [13,30]. In addition to the structural similarity between the

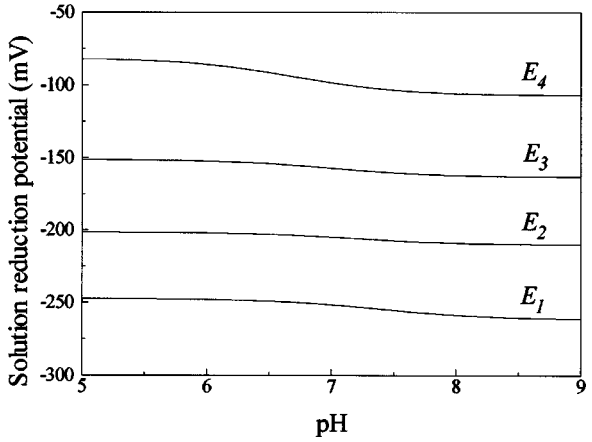

Figure 6 Macroscopic reduction potentials for *Sfc* calculated as a function of pH

The macroscopic reduction potentials were calculated using the parameters listed in Table 1 and are numbered according to each stage of oxidation.

haem cores, there is a high degree of sequence identity (42 %) and the macroscopic reduction potentials of the *Sfc* (Figure 6) are also similar to those of *Sffcc*$_3$ [31]. Based on all those observations, the results obtained for *Sfc* may be rationalized to propose a putative functional redox model for the *Sffcc*$_3$.

The crystal structure of *Sffcc*$_3$ reveals that haem IV is the closest (7.4 Å, edge-to-edge) haem group to the FAD cofactor [13]. Thus the lower reduction potential of haem IV favours the transfer of electrons to the FAD cofactor, in order that catalytic conversion of fumarate to succinate occurs. In fact, haem IV in the fully reduced and protonated *Sfc* has a microscopic reduction potential of -229 mV (Table 1), which is significantly lower than that observed for FAD of *Sffcc*$_3$ [31] and, consequently, a thermodynamically favourable electron transfer may occur from haem IV to FAD. After transferring the electron to FAD, haem IV becomes oxidized and the negative interaction involving this haem and haem III increases the potential of the latter by 42 mV (Table 1A). Thus the transfer of two electrons from the tetrahaem domain to the FAD involves a thermodynamically unfavourable electron transfer step from haem III to haem IV. However, haem III in *Sfc* still has a more negative reduction potential than FAD in *Sffcc*$_3$, and thus the overall electron transfer process is favourable. Furthermore, the reduction potentials of haems I and II are also more negative than haem III; thus a transfer of electrons from these haems to haem III is also thermodynamically favourable. Since the intramolecular electronic exchange between the redox cofactors is fast, and given the microscopic redox properties of *Sfc*, the tetrahaem domain of *Sffcc*$_3$ should allow a facile flow of electrons across its full length from haem I to haem IV to be donated to the FAD in the catalytic site.

As pointed out previously, within the cytochrome domain of *Sffcc*$_3$ one endergonic electron transfer step is included along the chain of redox centres. This is also found in the membrane-bound fumarate reductases [55,56], in hydrogenases [57] and in mitochondrial succinate dehydrogenases [58]. However, theoretical calculations indicate that this thermodynamic barrier presents no significant obstacle to fast electron transfer [57]. Furthermore, in *Sfc* the microscopic redox potentials of the haem groups are much more similar when compared with several cases reported in the literature, namely for membrane-bound fumarate reductases ([59] and references therein), hydrogenases [57,60], *Rhodopseudomonas viridis* cytochromes [57,61] and mitochondrial succinate dehydrogenases [58]. In *Sffcc*$_3$ a much smaller endergonic electron transfer step is needed for the electron transfer within the chain of redox cofactors. This advantage, coupled with short distances (3.9–8.0 Å, edge-to-edge) between the neighbouring redox cofactors [13], should lead to a very efficient electron transfer along the redox chain in *Sffcc*$_3$.

Although the physiological redox partners of *Sfc* are still unknown, the data presented in this work show that *Sfc* can act as an electron wire between its redox partners due to the linear spatial disposition and close proximity of the haem groups, and the thermodynamic properties that allow electrons to flow along the chain of haems in this protein.

We are very grateful to Professor António V. Xavier and Dr Teresa Catarino for helpful and fruitful discussions. This work was supported by a Fundação para a Ciência e a Tecnologia (FCT)-Portugal grant (POCTI/42902/QUI/2001) and doctoral fellowship (SFRH/5229/2001), and by a Conselho de Reitores das Universidades Portuguesas (CRUP)-Portugal grant (B20/01, B32/02).

REFERENCES

1 Lovley, D. R. (1991) Dissimilatory Fe(III) and Mn(IV) reduction. Microbiol. Rev. **55**, 259–287
2 Lovley, D. R. (1997) Microbial Fe(III) reduction in subsurface environments. FEMS Microbiol. Rev. **20**, 305–313
3 Thamdrup, B. (2000) Microbial manganese and iron reduction in aquatic sediments. Adv. Microb. Ecol. **16**, 41–84
4 Sharp, R. E., Moser, C. C., Rabanal, F. and Dutton, P. L. (1998) Design, synthesis, and characterization of a photoactivatable flavocytochrome molecular maquette. Proc. Natl. Acad. Sci. U.S.A. **95**, 10465–10470
5 Pettigrew, G. W. and Moore, G. R. (1987) Cytochromes *c*. Biological Aspects, in Springer Series in Molecular Biology (Rich, A., ed.), pp. 15–28, Springer-Verlag, Berlin
6 Moore, G. R. and Pettigrew, G. W. (1990) Cytochromes *c*. Evolutionary, Structural and Physicochemical Aspects, in Springer Series in Molecular Biology, pp. 13–25, 241–253 and 309–344, Springer-Verlag, Berlin
7 Sharp, R. E. and Chapman, S. K. (1999) Mechanisms for regulating electron transfer in multi-centre redox proteins. Biochim. Biophys. Acta **1432**, 143–158
8 Haser, R., Pierrot, M., Frey, M., Payan, F., Astier, J. P., Bruschi, M. and LeGall, J. (1979) Structure and sequence of the multihaem cytochrome c_3. Nature (London) **282**, 806–810
9 Magro, V., Pieulle, L., Forget, N., Guigliarelli, B., Petillot, Y. and Hatchikian, E. C. (1997) Further characterization of the two tetraheme cytochromes c_3 from *Desulfovibrio africanus*: nucleotide sequences, EPR spectroscopy and biological activity. Biochim. Biophys. Acta **1342**, 149–163
10 Simões, P., Matias, P. M., Morais, J., Wilson, K., Dauter, Z. and Carrondo, M. A. (1998) Refinement of the three-dimensional structures of cytochrome c_3 from *Desulfovibrio vulgaris* Hildenborough at 1.67 Å resolution and from *Desulfovibrio desulfuricans* ATCC 27774 at 1.6 Å resolution. Inorg. Chim. Acta **273**, 213–224
11 Brennan, L., Turner, D. L., Messias, A. C., Teodoro, M. L., LeGall, J., Santos, H. and Xavier, A. V. (2000) Structural basis for the network of functional cooperativities in cytochrome c_3 from *Desulfovibrio gigas*: solution structures of the oxidised and reduced states. J. Mol. Biol. **298**, 61–82
12 Leys, D., Tsapin, A. S., Nealson, K. H., Meyer, T. E., Cusanovich, M. A. and Beeumen, J. J. V. (1999) Structure and mechanism of the flavocytochrome c fumarate reductase of *Shewanella putrefaciens* MR-1. Nat. Struct. Biol. **6**, 1113–1117
13 Taylor, P., Pealing, S. L., Reid, G. A., Chapman, S. K. and Walkinshaw, M. D. (1999) Structural and mechanistic mapping of a unique fumarate reductase. Nat. Struct. Biol. **6**, 1108–1112
14 Deisenhofer, J., Epp, O., Sinning, I. and Michel, H. (1995) Crystallographic refinement at 2.3 Å resolution and refined model of the photosynthetic reaction centre from *Rhodopseudomonas viridis*. J. Mol. Biol. **246**, 429–457
15 Iverson, T. M., Arciero, D. M., Hsu, B. T., Logan, M. S., Hooper, A. B. and Rees, D. C. (1998) Haem packing motifs revealed by the crystal structure of the tetrahaem cytochrome c_{554} from *Nitrosomonas europeaea*. Nat. Struct. Biol. **5**, 1005–10012
16 Iverson, T. M., Arciero, D. M., Hooper, A. B. and Rees, D. C. (2001) High-resolution structures of the oxidized and reduced states of cytochrome c_{554} from *Nitrosomonas europaea*. J. Biol. Inorg. Chem. **6**, 390–397
17 Tsapin, A. I., Nealson, K. H., Meyers, T., Cusanovich, M. A., Van Beuumen, J., Crosby, L. D., Feinberg, B. A. and Zhang, C. (1996) Purification and properties of a low-redox-potential tetraheme cytochrome c_3 from *Shewanella putrefaciens*. J. Bacteriol. **178**, 6386–6388

18 Gordon, E. H. J., Pike, A. D., Hill, A. E., Cuthbertson, P. M., Chapman, S. K. and Reid, G. A. (2000) Identification and characterization of a novel cytochrome c_3 from *Shewanella frigidimarina* that is involved in Fe(III) respiration. Biochem. J. **349**, 153–158

19 Richardson, D. J. (2000) Bacterial respiration: a flexible process for a changing environment. Microbiology **146**, 551–571

20 Myers, C. R. and Nelson, K. H. (1988) Bacterial manganese reduction and growth with manganese oxide as the sole electron acceptor. Science **240**, 1319–1321

21 Myers, C. R. and Nelson, K. H. (1990) Respiration-linked proton translocation coupled to anaerobic reduction of manganese(IV) and iron(III) in *Shewanella putrefaciens* MR-1. J. Bacteriol. **172**, 6232–6238

22 Newman, D. K. and Kolter, R. A. (2000) A role for excreted quinines in extracellular electron transfer. Nature (London) **405**, 94–97

23 Childers, S. E., Ciufo, S. and Lovley, D. R. (2002) *Geobacter metallireducens* accesses insoluble Fe(III) oxide by chemotaxis. Nature (London) **416**, 767–769

24 Myers, C. R. and Myers, J. M. (1992) Localization of cytochromes to the outer membrane of anaerobically grown *Shewanella putrefaciens* MR-1. J. Bacteriol. **174**, 3429–3438

25 Myers, C. R. and Myers, J. M. (1997) Cloning and sequence of cymA, a gene encoding a tetrahaem cytochrome *c* required for reduction of iron(III), fumarate, and nitrate by *Shewanella putrefaciens* MR-1. J. Bacteriol. **179**, 1143–1152

26 Myers, C. R. and Myers, J. M. (1997) Outer membrane cytochromes of *Shewanella putrefaciens* MR-1: spectral analysis, and purification of the 83 kDa *c*-type cytochrome. Biochim. Biophys. Acta **1326**, 307–318

27 Myers, J. M. and Myers, C. R. (1998) Isolation and sequence of omcA, a gene encoding a decaheme outer membrane cytochrome *c* of *Shewanella putrefaciens* MR-1, and detection of omcA homologs in other strains of *S. putrefaciens*. Biochim. Biophys. Acta **1373**, 237–251

28 Beliaev, A. S. and Safarini, D. A. (1998) *Shewanella putrefaciens* mtrB encodes an outer membrane protein required for Fe(III) and Mn(IV) reduction. J. Bacteriol. **180**, 6292–6297

29 Field, S. J., Dobbin, P. S., Cheesman, M. R., Watmough, N. J., Thomson, A. J. and Richardson, D. J. (2000) Purification and magneto-optical spectroscopic characterization of cytoplasmic membrane and outer membrane multihaem *c*-type cytochromes from *Shewanella frigidimarina* NCIMB400. J. Biol. Chem. **275**, 8515–8522

30 Pessanha, M., Brennan, L., Xavier, A. V., Cuthbertson, P. M., Reid, G. A., Chapman, S. K., Turner, D. L. and Salgueiro, C. A. (2001) NMR structure of the haem core of a novel tetrahaem cytochrome isolated from *Shewanella frigidimarina*: identification of the haem-specific axial ligands and order of oxidation. FEBS Lett. **489**, 8–13

31 Turner, K. L., Doherty, M. K., Heering, H. A., Armstrong, F. A., Reid, G. A. and Chapman, S. K. (1999) Redox properties of flavocytochrome c_3 from *Shewanella frigidimarina* NCIMB400. Biochemistry **38**, 3302–3309

32 Einsle, O., Messerschmidt, A., Stach, P., Bourenkov, G. P., Bartunik, H. D., Huber, R. and Kroneck, P. M. (1999) Structure of cytochrome *c* nitrite reductase. Nature (London) **400**, 476–480

33 Igarashi, N., Moriyama, H., Fujiwara, T., Fukumori, Y. and Tanaka, N. (1997) The 2.8 Å structure of hydroxylamine oxidoreductase from a nitrifying chemoautotrophic bacterium, *Nitrosomonas europaea*. Nat. Struct. Biol. **4**, 276–284

34 Santos, H., Moura, J. J. G., Moura, I., LeGall, J. and Xavier, A. V. (1984) NMR studies of electron transfer mechanisms in a protein with interacting redox centres: *Desulfovibrio gigas* cytochrome c_3. Eur. J. Biochem. **141**, 283–296

35 Park, J.-S., Ohmura, T., Kano, K., Sagara, T., Niki, K., Kyogoku, Y. and Akutsu, H. (1996) Regulation of the redox order of four hemes by pH in cytochrome c_3 from *D. vulgaris* Miyazaki F. Biochim. Biophys. Acta **1293**, 45–54

36 Turner, D. L., Salgueiro, C. A., Catarino, T., LeGall, J. and Xavier, A. V. (1996) NMR studies of cooperativity in the tetrahaem cytochrome c_3 from *Desulfovibrio vulgaris*. Eur. J. Biochem. **241**, 723–731

37 Salgueiro, C. A., Turner, D. L., LeGall, J. and Xavier, A. V. (1997) Reevaluation of the redox-Bohr cooperativity in tetrahaem *Desulfovibrio vulgaris* (Miyazaki F) cytochrome c_3. J. Biol. Inorg. Chem. **2**, 343–349

38 Salgueiro, C. A., da Costa, P. N., Turner, D. L., Messias, A. C., van Dongen, W. M., Saraiva, L. M. and Xavier, A. V. (2001) Effect of hydrogen-bond networks in controlling reduction potentials in *Desulfovibrio vulgaris* (Hildenborough) cytochrome c_3 probed by site-specific mutagenesis. Biochemistry **40**, 9709–9716

39 Louro, R. O., Catarino, T., Turner, D. L., Piçarra-Pereira, M. A., Pacheco, I., LeGall, J. and Xavier, A. V. (1998) Functional and mechanistic studies of cytochrome c_3 from *Desulfovibrio gigas*: thermodynamics of a ''proton thruster''. Biochemistry **37**, 15808–15815

40 Louro, R. O., Catarino, T., LeGall, J., Turner, D. L. and Xavier, A. V. (2001) Cooperativity between electrons and protons in a monomeric cytochrome c_3: the importance of mechano-chemical coupling for energy transduction. Chembiochem. **2**, 831–837

41 Saraiva, L. M., Salgueiro, C. A., da Costa, P. N., Messias, A. C., LeGall, J., van Dongen, W. M. A. M. and Xavier, A. V. (1998) Replacement of lysine 45 by uncharged residues modulates the redox-Bohr effect in tetraheme cytochrome c_3 of *Desulfovibrio vulgaris* (Hildenborough). Biochemistry **37**, 12160–12165

42 Pereira, P. M., Pacheco, I., Turner, D. L. and Louro, R. O. (2002) Structure-function relationship in type II cytochrome c_3 from *Desulfovibrio africanus*: a novel function in a familiar haem core. J. Biol. Inorg. Chem. **7**, 815–822

43 Louro, R. O., Catarino, T., Salgueiro, C. A., LeGall, J. and Xavier, A. V. (1996) Redox-Bohr effect in the tetrahaem cytochrome c_3 from *Desulfovibrio vulgaris*: a model for energy transduction mechanisms. J. Biol. Inorg. Chem. **1**, 34–38

44 Reis, C., Louro, R. O., Pacheco, I., Catarino, T., Turner, D. L. and Xavier, A. V. (2002) Redox-Bohr effect in the nine haem cytochrome from *Desulfovibrio desulfuricans* 27774. Inorg. Chim. Acta **339**, 248–252

45 Delgado, R., Fraústo da Silva, J. J. R., Amorim, M. T. S., Cabral, M. F., Chaves, S. and Costa, J. (1991) Dissociation constants of Bronsted acids in D_2O and H_2O: studies on polyaza and polyoxapolyaza macrocycles and a general correlation. Anal. Chim. Acta **245**, 271–282

46 Bartels, C., Xia, T., Billeter, M., Güntert, P. and Wüthrich, K. (1995) The program XEASY for computer-supported NMR spectral-analysis of biological macromolecules. J. Biomol. NMR **6**, 1–10

47 Dutton, P. L. (1978) Redox potentiometry: determination of mid-point potentials of oxidation-reduction components of biological electron-transfer systems. Methods Enzymol. **54**, 411–435

48 Catarino, T. (1998) Thermodynamic and Kinetic Modelling of the Redox Properties of Tetrahaem Cytochromes c_3, Ph.D. Thesis, Instituto de Tecnologia Química e Biológica, Universidade Nova de Lisboa, Lisbon

49 Correia, I. J., Paquete, C. M., Louro, R. O., Catarino, T., Turner, D. L. and Xavier, A. V. (2002) Thermodynamic and kinetic characterization of trihaem cytochrome c_3 from *Desulfuromonas acetoxidans*. Eur. J. Biochem. **269**, 1–8

50 Salgueiro, C. A., Turner, D. L., Santos, H., LeGall, J. and Xavier, A. V. (1992) Assignment of the redox potentials to the four haems in *Desulfovibrio vulgaris* cytochrome c_3 by 2D-NMR. FEBS Lett. **314**, 155–158

51 Dolla, A., Blanchard, L., Guerlesquin, F. and Bruschi, M. (1994) The protein moiety modulates the redox potential in cytochromes *c*. Biochimie **76**, 471–479

52 Lee, K. K., Fitch, C. A. and Garcia-Moreno, B. (2002) Distance dependence and salt sensitivity of pairwise, coulombic interactions in a protein. Protein Sci. **11**, 1004–1016

53 Creighton, T. E. (1994) Proteins – Structure and Molecular Properties, W.H. Freedman and Company, New York

54 Leys, D., Meyer, T. E., Tsapin, A. S., Nealson, K. H., Cusanovich, M. A. and Beeumen, J. J. V. (2002) Crystal structures at atomic resolution reveal the novel concept of 'electron-harvesting' as a role for the small tetrahaem cytochrome *c*. J. Biol. Chem. **277**, 35703–35711

55 Iverson, T. M., Chavez, C. L., Cecchini, G. and Rees, D. C. (1999) Structure of the *Escherichia coli* fumarate reductase respiratory complex. Science **284**, 1961–1966

56 Ohnishi, T., Moser, C. C., Page, C. C., Dutton, P. L. and Yano, T. (2000) Simple redox-linked proton-transfer design: new insights from structures of quinol-fumarate reductase. Structure Fold. Des. **8**, R23–R32

57 Page, C. C., Moser, C. C., Chen, X. and Dutton, P. L. (1999) Natural engineering principles of electron tunnelling in biological oxidation-reduction. Nature (London) **402**, 47–52

58 Dutton, P. L., Chen, X., Page, C. C., Huang, S., Onishi, T. and Moser, C. C. (1998) Respiratory electron transfer proteins, in Biological Electron Transfer Chains: Genetics, Composition and Mode of Operation (Canters, G. W. and Vijgenboom, E., eds.), pp. 3–8, Kluwer Academic Publishers, Dordrecht

59 Cecchini, G., Schroder, I., Gunsalus, R. P. and Maklashina, E. (2002) Succinate dehydrogenase and fumarate reductase from *Escherichia coli*. Biochim. Biophys. Acta **1553**, 140–157

60 Teixeira, M., Moura, I., Xavier, A. V., Moura, J. J., LeGall, J., DerVartanian, D. V., Peck, Jr, H. D. and Huynh, B. H. (1989) Redox intermediates of *Desulfovibrio gigas* [NiFe] hydrogenase generated under hydrogen. Mossbauer and EPR characterization of the metal centers. J. Biol. Chem. **264**, 16435–16450

61 Chen, I., Mathis, P., Koepke, J. and Michel, H. (2000) Uphill electron transfer in the tetrahaem cytochrome subunit of the *Rhodopseudomonas viridis* photosynthetic reaction centre: evidence from site-directed mutagenesis. Biochemistry **39**, 3592–3602

Received 6 September 2002/31 October 2002; accepted 4 November 2002
Published as BJ Immediate Publication 4 November 2002, DOI 10.1042/BJ20021408